Hole spin relaxation in quantum dots

L. M. Woods,[1,*] T. L. Reinecke,[1] and R. Kotlyar[2]
[1]*Naval Research Laboratory, Washington DC 20375, USA*
[2]*Intel Corporation, Hillsboro, Oregon 97214, USA*
(Received 28 August 2003; published 22 March 2004)

We present results for relaxation of the spin of a hole in a cylindrical quantum dot due to acoustic phonon assisted spin flips at low temperatures with an applied magnetic field. The hole dispersion is calculated by numerical diagonalization of the Luttinger Hamiltonian and applying perturbation theory with respect to the magnetic field, and the hole-phonon coupling is described by the Bir-Pikus Hamiltonian. We find that the decoherence time for hole spins for dots $\lesssim 20$ nm is on the order of 10^{-8} s. This is several orders smaller than the decoherence time due to phonon assisted processes for electron spins in similar dots and is comparable to the total decoherence time of an electron spin in a quantum dot, which is controlled by the hyperfine interaction with nuclei. We obtain the dependence of the relaxation rate of the hole spin on dot size and hole mass.

DOI: 10.1103/PhysRevB.69.125330 PACS number(s): 63.20.Ls, 63.22.+m, 68.65.Hb, 71.15.−m

I. INTRODUCTION

Recently considerable interest has been devoted to developing a theory for the relaxation of an electron spin localized in a quantum dot (QD).[1–3] The problem is of importance for processing and transferring information coherently in structures of interest for quantum computation. It has been found that two processes are responsible for the loss of coherence of the electron spin. First, phonon assisted spin flips mediated by spin-orbit coupling give relaxation rates on the order of 10^{-4} s in QD's where the dominant phonon scattering arises from piezoelectric coupling[1] and interface motion.[2] Second, the spatially inhomogeneous coupling of nuclei via the hyperfine interaction to the electron wave function gives an effective dephasing time on the order of 10^{-6} s (Ref. 3).

The valence band in typical III–V semiconductors has *p* symmetry and does not couple to nuclei. Thus the potentially slower relaxation due to phonons is expected to dominate. Hole spin relaxation has been studied in bulk semiconductors[4] and in quantum wells.[5,6] There, relaxation typically occurs by elastic phonon processes mediated by spin-orbit coupling and gives rapid rates on the order of ps and ns, respectively, due to strong phonon scattering of holes. In dots, on the other hand, the hole states are discrete, and thus phonon induced scattering involves inelastic processes. Therefore hole spin relaxation could be slow in QD's, and holes might become attractive candidates as carriers of quantum information (''qubits''). To date, however, hole relaxation in quantum dots remains poorly understood. In part this is because of the theoretical challenges resulting from the coupling of the valence bands. We address this problem here.

We study the relaxation of a hole spin localized in a QD due to scattering with acoustic phonons in the presence of a magnetic field. The formulation here can represent a range of QD systems. To be definite, calculations are done for a QD in cylindrical form with a lateral size larger than its vertical extension. This model represents deep etched dots[7] well, and it would also represent, at least qualitatively, dots formed by Stranski-Krastanov growth.[8] Here we perform a numerical diagonalization of the 4×4 Luttinger Hamiltonian to obtain the valence subbands and energy dispersions. This includes the interaction between the light and heavy holes in the dot, which is known to modify the spectrum significantly. The magnetic field is included perturbatively.

In zincblende semiconductors the holes have *p*-type symmetry. In nanostructures there can be strains at interfaces. In addition acoustic phonons involve dynamic strains. Here we use a Bir-Pikus Hamiltonian as a general representation of the valence band with strains. We calculate the scattering between the two bands highest in energy with this Hamiltonian, and we also find the dependences on physical factors of interest, including size, magnetic field, mass, and temperature.

II. VALENCE SUBBANDS AND HOLE-PHONON COUPLING

We consider a quantum dot (QD) obtained by deep etching of an InGaAs/GaAs quantum well. The valence subbands are studied by a standard four-band $\mathbf{k}\cdot\mathbf{p}$ effective-mass approach,[9] which allows us to treat the interaction between light and heavy holes. In the effective-mass $\mathbf{k}\cdot\mathbf{p}$ method the dynamics of the holes is determined by its structure at the zone edge $\mathbf{k}=0$, and only small terms (up to $\mathbf{k}^2$) are present in the Hamiltonian. The total wave function $\Psi_{\mathbf{k}}$ is represented as a product of a Bloch function $u_{j\mathbf{k}=0}$ and an envelope function $\psi_{j\mathbf{k}}$, and therefore $\Psi_{\mathbf{k}}=\Sigma_j \psi_{j\mathbf{k}} u_{j\mathbf{k}=0}$, where j runs over all bands. The basis states $u_{j\mathbf{k}=0}$ used here have total angular momentum $J=\frac{3}{2}$ with projections $m_J=\pm\frac{3}{2}$ for the heavy holes and $m_J=\pm\frac{1}{2}$ for the light holes. In this basis the Hamiltonian has the form[10]

$$H=\begin{pmatrix} P+Q-\frac{3}{2}\kappa\mu_0 B & S & R & 0 \\ S^+ & P-Q-\frac{1}{2}\kappa\mu_0 B-\Lambda & 0 & R \\ R^+ & 0 & P-Q+\frac{1}{2}\kappa\mu_0 B-\Lambda & -S \\ 0 & R^+ & -S^+ & P+Q+\frac{3}{2}\kappa\mu_0 B \end{pmatrix}, \tag{1}$$

which describes the hole band mixing. Here

$$P\pm Q=-(\gamma_1\pm\gamma_2)\frac{\hbar^2k_\perp^2}{2m_0}-(\gamma_1\mp 2\gamma_2)\frac{\hbar^2k_z^2}{2m_0}, \tag{2}$$

$$S=2\sqrt{3}\gamma_2\frac{\hbar^2k_zk_\perp}{2m_0}, \tag{3}$$

$$R=\sqrt{3}\gamma_2\frac{\hbar^2k_\perp^2}{2m_0}. \tag{4}$$

The coupling between the conduction electron and the hole bands is smaller, and it is not included here. We use the spherical approximation[11] for the Luttinger γ coefficients. For the wave vector the conventions are $k_\perp^2=k_x^2+k_y^2$ and $k_\pm=k_x\pm ik_y$. The magnetic field B is along z axis, and it enters the Hamiltonian through the diagonal Zeeman terms and through the magnetic-field dependence of $\mathbf{k}=-i\Delta+e\mathbf{A}/\hbar$, where $\mathbf{A}$ is the vector potential. A parameter Λ is included representing the spin-independent strain splitting between the heavy- and light-hole bands that originates from a lattice mismatch at the interfaces[11] and it gives rise to the uniaxial strain.

For the structures considered here the three-dimensional confinement can be described by infinite wall potentials in the lateral direction with d/2 the radius of the dot and a confining potential along the z direction

$$V_z=\begin{cases} 0, & |z|\leqslant c/2 \\ V_0, & |z|>c/2. \end{cases} \tag{5}$$

Here $V_0=-69.2$ meV is for the heavy-hole bands, and $-(69.2-\Lambda)$ meV for the light-hole bands, which are chosen from $In_{0.1}Ga_{0.9}As$, and Λ is taken to be $\Lambda=40$ meV (Ref. 13). The well width c is chosen to be 5 nm, and the QD is in a cylindrical form.

The hole-phonon interaction including the effects of strain from phonons is given by the Bir-Pikus Hamiltonian.[12] The components of the strain tensor ϵ in terms of normal-mode coordinates are

$$\epsilon_{ij}=\sum_{\mathbf{Q}}\frac{i}{2}\sqrt{\frac{\hbar}{2\rho\omega_{\mathbf{Q}}}}(Q_i\hat{\eta}_j+Q_j\hat{\eta}_i)e^{i\mathbf{Q}\cdot\mathbf{r}}. \tag{6}$$

Here ρ is the mass density of the material, $\mathbf{Q}$ is the phonon wave vector, $\hat{\eta}$ is the phonon polarization, and $\omega_{\mathbf{Q}}$ is the phonon frequency.

The form of the hole-phonon interaction is similar to that in Eq. (1) but with matrix elements

$$P_{\mathbf{Q}}=D_dTr(\epsilon), \tag{7}$$

$$Q_{\mathbf{Q}}=-\frac{2}{3}D_u(\epsilon_{xx}+\epsilon_{yy}-2\epsilon_{zz}), \tag{8}$$

$$R_{\mathbf{Q}}=\frac{1}{\sqrt{3}}D_u(\epsilon_{xx}-\epsilon_{yy})-i\frac{2}{\sqrt{3}}D_u'\epsilon_{xy}, \tag{9}$$

$$S_{\mathbf{Q}}=-\frac{2}{\sqrt{3}}D_u'(\epsilon_{zx}-i\epsilon_{zy}), \tag{10}$$

where $D_d=8.9$ eV, $D_u=5.4$ eV, and $D_u'=1.98$ eV are the deformation potential constants characteristic of InGaAs heterostructures.[16] The matrix elements $P_{\mathbf{Q}}$, $Q_{\mathbf{Q}}$, $R_{\mathbf{Q}}$, and $S_{\mathbf{Q}}$ are expressed in terms of the strain tensor components ϵ_{ij}.

The hole-phonon scattering rate is calculated from the Fermi golden rule

$$\Gamma=\frac{2}{(2\pi)^3\hbar}\int d^3Q[N_{\mathbf{Q}}+\tfrac{1}{2}\pm\tfrac{1}{2}]|M_{\mathbf{Q}}|^2\delta(\hbar\omega_{\mathbf{Q}}-\Delta E), \tag{11}$$

where $N_{\mathbf{Q}}$ is the phonon occupation factor, ΔE is the energy difference between the two lowest hole states, and $M_{\mathbf{Q}}$ is the corresponding matrix element. Here $M_{\mathbf{Q}}=\langle\psi_{init}|H_{\mathbf{Q}}|\psi_{fin}\rangle$ with $H_{\mathbf{Q}}$ the matrix for the hole-phonon interaction and $|\psi_{init,fin}\rangle$ are the initial and final hole states.

In order to calculate the hole-phonon scattering, the hole wave functions are needed. For that purpose the Hamiltonian H from Eq. (1) must be diagonalized. In general this is a formidable task, and therefore we apply a two-step perturbation theory. The first perturbation is for small magnetic field B. Thus we separate the Hamiltonian from Eq. (1) into $H=H_0+H_B$, where H_0 is for $B=0$ and H_B contains all the terms with the magnetic field B.

To describe the valence-band states the valence-subband mixing must be taken into account in solving H_0. Since the

system has cylindrical symmetry, the Hamiltonian commutes with the operator F_z of the projection of the total angular momentum $\mathbf{F}=\mathbf{L}+\mathbf{J}$, where $\mathbf{J}$ is the Bloch angular momentum and $\mathbf{L}$ is the envelope angular momentum. H_0 is diagonalized numerically for a given F_z using the following basis of envelope functions:[13]

$$\psi_{F_z\pm 3/2}=\frac{e^{i(F_z\pm 3/2)}}{\sqrt{2\pi}}R_{F_z\pm 3/2}(\rho)Z_{F_z\pm 3/2}(z), \quad (12)$$

$$\psi_{F_z\pm 1/2}=\frac{e^{i(F_z\pm 1/2)}}{\sqrt{2\pi}}R_{F_z\pm 1/2}(\rho)Z_{F_z\pm 1/2}(z), \quad (13)$$

where the radial functions $R(\rho)$ satisfy the boundary condition $R(d/2)=0$ and d is the diameter of the dot. The radial functions are expanded in the orthonormal basis set of Bessel functions,

$$R_{m_j}=\sum_i a_i^{m_j}J_{m_j}\left(\beta_{m_j}^i\frac{2\rho}{d}\right) \quad (14)$$

with $\beta_{m_j}^i$ the ith root of the Bessel function J_{m_j}.

The function along the z direction $Z(z)$ is expanded in an orthonormal basis set as

$$Z_{m_j}=\sum_i b_i^{m_j}\xi_i^{m_j}(z), \quad (15)$$

where $\xi_i(z)$ are the solutions of the Schrödinger equation in the vertical direction

$$\left[\frac{\hbar^2k_z^2}{2m_z}+V(z)\right]\xi_i(z)=E_{i,z}\xi_i(z). \quad (16)$$

This expansion works for heterostructures with materials having similar material characteristics. The small differences in the effective masses within and outside of the quantum dot are neglected. To treat the continuum states and the bound states of the vertical well, the scheme of Ando[14] is used by enclosing the dot into a large box with 100 times larger z extension. The eigenstates $Z(z)$ are characterized by the index i for each band and by ''parity.'' The definite parity is a consequence of the symmetric form of the potential well.

In principle, one can perform the direct numerical diagonalization of the total Hamiltonian for $B=0$. H_0 is diagonalized in the above basis set for a specific quantum number F_z. For realistic quantum dots, however, the direct numerical evaluation of the matrix from Eq. (1) generally requires the expansion of the wave functions in large basis sets and diagonalization of very large matrices in order to obtain convergence.[13] To overcome this we apply a second expansion in H_0 with respect to the parallel wave vector $\mathbf{k}_\perp$ as in Ref. 13 where the lateral dimension of the dot is much greater than the vertical dimension. This method is especially useful for systems with lower dimensions. Then, the Hamiltonian for zero magnetic field is

$$H_0=H_0(k_\perp=0)+H', \quad (17)$$

$$H'=\frac{\hbar^2}{2m_0}[\hat{h}_+k_+ +\hat{h}_-k_- +\hat{h}_{2+}k_+^2+\hat{h}_{2-}k_-^2], \quad (18)$$

where $\hat{h}_{+,-}$ and $\hat{h}_{2+,2-}$ can be found from the Hamiltonian in Eq. (1) and k_x, k_y are evaluated by π/d, where d is the lateral size of the dot. The energy spectrum and valence bands are calculated by treating H' perturbatively, using the method in Ref. 13 and they are characterized by the indices n_ρ, n_z, and parity. The unperturbed wave functions are those in Eqs. (12) and (13)

Next, we apply perturbation theory with respect to the magnetic field through H_B for B small. The wave function can be written as

$$\psi_{F_z\pm 3/2}=\psi^0_{F_z\pm 3/2}+\alpha_{1(2)}\psi^0_{F_z-1/2}+\beta_{1(2)}\psi^0_{F_z+1/2}, \quad (19)$$

$$\psi_{F_z\pm 1/2}=\psi^0_{F_z\pm 1/2}+\alpha_{3(4)}\psi^0_{F_z-3/2}+\beta_{3(4)}\psi^0_{F_z+3/2}, \quad (20)$$

where the α and β coefficients are determined from H_B and they are all $\sim\hbar eB/2m_0$. The energies $E_{F_z\pm 3/2}$ and $E_{F_z\pm 1/2}$ are calculated up to the first order in the magnetic field B.

III. SCATTERING RATES FOR HOLE SPINS

To calculate the rate of the hole scattering between spin states we first determine the valence bands highest in energy using the method described in Sec. II. The calculation is done by numerical diagonalization of H_0 using the perturbative approach described above. For the QD's studied here the two bands highest in energy preserve their heavy- and light-hole character, and they are degenerate for $B=0$ with $m_j=\pm 3/2$. The perturbation H_B causes a splitting between the $m_j=3/2$ and $m_j=-3/2$ bands, and the character of the bands becomes a mixture of heavy and light holes. The highest in energy bands have quantum numbers $F_z=-3/2$ for $m_j=3/2$ and $F_z=3/2$ for $m_j=3/2$.

The transitions of interest for hole dephasing by spin flips are

$$M_{\mathbf{Q}}=\langle\psi_{F_z=3/2,m_j=-3/2,A}|H_{\mathbf{Q}}|\psi_{F_z=-3/2,m_j=3/2,B}\rangle, \quad (21)$$

where A and B stand for the parity of the bands. This expression has several terms due to the complex nature of the hole-phonon coupling $H_{\mathbf{Q}}$—Eqs. (1), (7)–(10).

The scattering rates are calculated using the Fermi golden rule and the matrix element for the lowest transition from Eq. (21). Analytical results can be obtained if we consider the limit of small phonon wave vector $\mathbf{Q}$ in the exponential factor $e^{i\mathbf{Q}\cdot\mathbf{r}}\approx(1+i\mathbf{Q}\cdot\mathbf{r})$ from the strain tensor ϵ. We have examined contributions from all types of acoustic phonon polarizations—longitudinal (LA) $\hat{\eta}_i=Q_i/Q$ and the two transverse (TA) $\hat{\eta}_{t1}=(Q_xQ_z,Q_yQ_z,-Q_\perp^2)/QQ_\perp$ and $\hat{\eta}_{t2}=(Q_y,-Q_x,0)/Q_\perp$, where $Q=\sqrt{Q_x^2+Q_y^2+Q_z^2}$ and $Q_\perp=\sqrt{Q_x^2+Q_y^2}$. The result for the scattering rates are

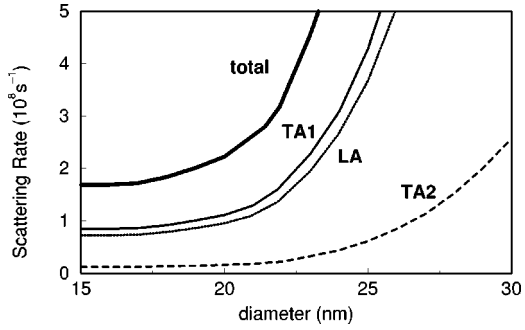

FIG. 1. Scattering rate for a cylindrical quantum dot with $c=5$ nm along the z direction and magnetic field $B=1$ T. The contributions from longitudinal acoustic phonons are denoted as LA, and those from the two transverse acoustic phonons as TA1 and TA2.

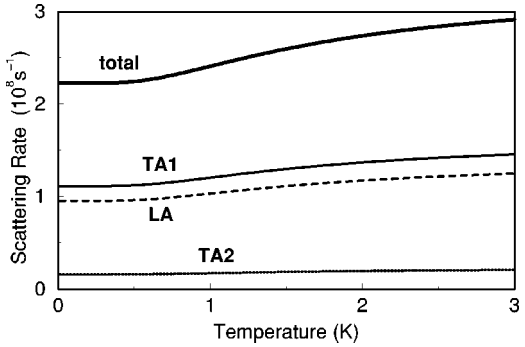

FIG. 2. Scattering rate for a cylindrical quantum dot with a diameter $d=20$ nm and $c=5$ nm as a function of temperature at $B=1$ T.

$$\Gamma = \frac{2\pi}{\hbar}\left[\sqrt{3}\,\gamma_2 \frac{\hbar e B}{2m_0 \Delta E}\,\frac{1}{\gamma_{hh}}\right]^2 \left(\frac{d}{2c}\right)^4 \times K \frac{D_u^2 + D_u'^2}{2\rho \bar{s}^2}\left(\frac{3\kappa\mu_0 B}{\hbar \bar{s}}\right)^5 x_i, \tag{22}$$

where $\Delta E = (E^0_{F_z=3/2,m_j=-3/2} - E^0_{F_z=3/2,m_j=-1/2})$ is the energy difference between the heavy and light holes for $B=0$. $\gamma_{hh} = \sqrt{2m_z^{hh}/\hbar^2 (V_0^{hh} - |E_z|)}$ with appropriate parameters for the heavy-hole subband. $K=1.882$ is a numerical factor obtained from the numerical diagonalization of the hole bands, and $\bar{s}$ is the sound velocity of InGaAs. The parameter $x_i = \frac{32}{35}, \frac{16}{105}, \frac{16}{15}$ for LA, TA1, and TA2 polarizations.

Equation (22) for spin relaxation rates allows us to determine the dependences on several physical parameters. From Eq. (22) the scattering rate is proportional to B^7. One is also able to see how the size of the QD affects Γ. The dependence on the lateral size comes from the d^4 and ΔE^{-2} parameters. The relaxation rate as a function of the dot diameter is shown in Fig. 1. The figure shows that after a diameter $d_0 \sim 20$ nm the scattering starts to increase nonlinearly leading to a nonlinear decrease of the coherence time. Below d_0 the rate is nearly a constant with a coherence time $\sim \mu s$. For the QD's studied here the two bands closest to the Fermi level preserve their heavy- and light-hole character, and the bands closest to E_F are degenerate for $B=0$ with $m_j = \pm 3/2$.

Figure 1 also shows that both the longitudinal and transverse polarizations are important with the TA scattering rate slightly larger. The scattering rates will increase at small diameters due to coupling to interfrace motion,[2,15] but these effects are not included here. Holes can interact with the LA phonons through the $P_{\mathbf{Q}}$, $Q_{\mathbf{Q}}$, and $R_{\mathbf{Q}}$ terms from the Bir-Pikus Hamiltonian. The interaction with the TA phonons comes from the terms $R_{\mathbf{Q}}$ and $S_{\mathbf{Q}}$ through the ϵ_{xy}, ϵ_{yz}, and ϵ_{xz} components of the strain tensor. The height of the dot, c, enters γ_{hh}. Here we use $c=5$ nm, and it is not changed in the calculation.

A comparison can be made with the phonon induced relaxation rates of an electron spin in a QD.[2] For an electron spin the relaxation rate is about 4 orders smaller than the rate for holes with lowest value for electrons on the order of 10^{-3}–10^{-4} s^{-1}. The electron scattering rate $\sim R^4$, where R is the radius of the QD (Ref. 2) and it goes as $\sim m_{el}^4$. The explicit dependences of Γ on size and mass is difficult to obtain for the holes because of the complicated diagonalization procedure. The radial mass is contained in ΔE and K through the numerical diagonalization. The mass along z axis is contained in γ_{hh} and K. For the sake of argument, if we take the hole energy to have a similar size and mass dependences as the electron energy, $E \sim 1/mR^2$, and use Eq. (22) we see that the hole scattering rate is $\sim m_\perp^2/m_z$ and $\sim R^8$. Since the electron mass is much less than the hole mass, the electron will have much slower relaxation than the hole. This could explain the dramatic difference in the value for the decoherence time for the electron ($\sim 10^{-3}$–10^{-4} s) and that for the hole ($\sim 10^{-8}$ s). In general the coherence time is longer for smaller dots for both holes and electrons.

We give the scattering as a function of temperature in Fig. 2. The temperature dependence comes from the phonon occupation factor $N_{\mathbf{Q}}$ in Γ in Eq. (11). The scattering rate is temperature independent up to $T \sim 0.5$ K. For higher T it increases linearly with T from $N_{\mathbf{Q}}$.

IV. DISCUSSION

In this paper we have given calculations of the scattering rates for relaxation of holes in cylindrical (deep etched) quantum dots due to the emission and absorption of acoustic phonons via the deformation potential interaction mediated by the spin-orbit interaction described by the Bir-Pikus Hamiltonian. A magnetic field is applied in the z direction. The Luttinger Hamiltonian was solved by numerical diagonalization for $B=0$, and the magnetic field is introduced with perturbation theory. In this way we determine the valence bands closest to the Fermi level and their energies.

The Bir-Pikus Hamiltonian for strained structures is used

to calculate the hole-phonon relaxation rates. The calculation includes both longitudinal and transverse acoustic phonons. The relaxation rates as functions of magnetic field, lateral size of the dot and temperature were determined. We find that the decoherence time due to hole relaxation is lower for smaller dots and for dots $\lesssim 20$ nm dots is of the order of 10^{-8} s. Corresponding spin-flip rates for electrons in quantum dots due to phonon scattering were found to be several orders of magnitude smaller.

This work was supported in part by the U.S. Office of Naval Research and by the DARPA QuIST program. One of us (L.M.W.) acknowledges an NRC/NRL Research Associateship.

*Present address: Department of Physics, University of South Florida, Tampa, FL 33620.

[1] A.V. Khaetskii and Y.V. Nazarov, Phys. Rev. B **61**, 12 639 (2000); **64**, 125316 (2001).

[2] L.M. Woods, T.L. Reinecke, and Y. Lyanda-Geller, Phys. Rev. B **66**, 161318 (2002).

[3] I.A. Merkulov, Al.L. Efros, and M. Rosen, Phys. Rev. B **65**, 205309 (2002); A.V. Khaetskii, D. Loss, and L. Glazman, Phys. Rev. Lett. **88**, 186802 (2002); J. Schliemann, A.V. Khaetskii, and D. Loss, Phys. Rev. B **66**, 245303 (2002); L. M. Woods and T. L. Reinecke (unpublished).

[4] J.M. Hinckley and J. Singh, Phys. Rev. B **41**, 2912 (1990).

[5] G. Sun, L. Friedman, and R.A. Soref, Phys. Rev. B **62**, 8114 (2000).

[6] Z. Ikonic, P. Harrison, and R.W. Kelsall, Phys. Rev. B **64**, 245311 (2001).

[7] R. Steffen, T. Koch, J. Oshinowo, F. Faller, and A. Forchel, Appl. Phys. Lett. **68**, 223 (1996).

[8] M. Grundmann *et al.*, Phys. Rev. Lett. **74**, 4043 (1995).

[9] J.M. Luttinger, Phys. Rev. **102**, 1030 (1959).

[10] T. Darnhofer, U. Rössler, and D.A. Broido, Phys. Rev. B **53**, 13 631 (1996).

[11] The Luttinger parameters are $\gamma_1 = 7.65$, $\bar{\gamma}_2 = 2.41$, and $\bar{\gamma}_3 = 3.28$. In the spherical-approximation $\gamma_2 = (\bar{\gamma}_2 + \bar{\gamma}_3)/2$. The other Luttinger parameter is $\kappa = 1.2$.

[12] G.L. Bir and G.E. Pikus, *Symmetry and Strain-Induced Effects in Semiconductors* (Wiley, New York, 1974).

[13] R. Kotlyar, T.L. Reinecke, M. Bayer, and A. Forchel, Phys. Rev. B **63**, 085310 (2001); R. Kotlyar, T. L. Reinecke, M. Bayer, T. Gutbrod, and A. Forchel (unpublished).

[14] T. Ando, J. Phys. Soc. Jpn. **54**, 1528 (1985).

[15] P.A. Knipp and T.L. Reinecke, Phys. Rev. B **48**, 12 338 (1993).

[16] F.H. Pollack and M. Cardona, Phys. Rev. **172**, 816 (1968).